

Published in final edited form as:

*Nat Ecol Evol.* 2017 November ; 1(11): 1716–1721. doi:10.1038/s41559-017-0311-7.

## Metals promote sequences of the reverse Krebs cycle

Kamila B. Muchowska, Sreejith J. Varma, Elodie Chevallot-Beroux, Lucas Lethuillier-Karl, Guang Li, and Joseph Moran\*

Université de Strasbourg, CNRS, ISIS UMR 7006, F-67000 Strasbourg, France

### Abstract

The rTCA cycle (also known as the reverse Krebs cycle) is a central anabolic biochemical pathway whose origins are proposed to trace back to geochemistry, long before the advent of enzymes, RNA or cells, and whose imprint still remains intimately embedded in the structure of core metabolism. If it existed, a primordial version of the rTCA cycle would necessarily have been catalyzed by naturally occurring minerals at the earliest stage of the transition from geochemistry to biochemistry. Here we report non-enzymatic promotion of multiple reactions of the rTCA cycle in consecutive sequence, whereby 6 of its 11 reactions are promoted by  $Zn^{2+}$ ,  $Cr^{3+}$  and  $Fe^0$  in an acidic aqueous solution. Two distinct three-reaction sequences can be achieved under a common set of conditions. Selectivity is observed for reduction reactions producing rTCA cycle intermediates compared to those leading off-cycle. Reductive amination of ketoacids to furnish amino acids is observed under similar conditions. The emerging reaction network supports the feasibility of primitive anabolism in an acidic, metal-rich reducing environment.

Life is inextricably linked to metabolism, a complex web of chemical reactions that build up (anabolize) and break down (catabolize) biomolecules. At the earliest stages of prebiotic chemistry at the origin of life, before the advent of enzymes or cells, synthetic chemical pathways must have acted to build molecular complexity from simpler starting materials.<sup>1,2</sup> However, debate exists over whether such a proto-anabolism “must generally be different from the underlying chemistry used in biology”<sup>3</sup> or whether it is recapitulated in extant anabolic pathways.<sup>4–9</sup> The former philosophy has inspired masterful syntheses of crucial biological molecules using chemical building blocks and custom-made synthetic routes that bear little resemblance to those used by life’s anabolic pathways. Though this approach is important, it inevitably leaves a vast gulf between the purported prebiotic chemistry and the biochemistry it ultimately aims to explain.<sup>10</sup> An alternative view is that primitive forms of

Users may view, print, copy, and download text and data-mine the content in such documents, for the purposes of academic research, subject always to the full Conditions of use:[http://www.nature.com/authors/editorial\\_policies/license.html#terms](http://www.nature.com/authors/editorial_policies/license.html#terms)

Correspondence should be addressed to J.M. ([moran@unistra.fr](mailto:moran@unistra.fr)).

#### Author contributions

J.M. supervised the research and the other authors performed the experiments. All the authors contributed intellectually throughout the project. J.M. wrote the paper and K.B.M assembled the Supplementary Information, additionally incorporating data from S.J.V, E.C.-B. and L.L.-K. Important preliminary experiments were carried out by G.L.

#### Competing financial interests

The authors declare no competing financial interests.

**Data availability.** The authors declare that the data supporting the findings of this study are available within the paper’s Supplementary Information files.

certain existing biological anabolic pathways could have originated spontaneously from geochemistry through naturally occurring catalysts before the existence of enzymes, RNA or cells – a parsimonious explanation for the emergence and organization of biochemistry. Indeed, Ralser and coworkers have demonstrated that several catabolic pathways, including most of the oxidative TCA cycle, are promoted without enzymes simply by using  $\text{Fe}^{2+}$  as a catalyst and/or peroxydisulfate ions as an oxidizing agent.<sup>11–13</sup> In contrast, non-enzymatic catalysis of extant *anabolic* pathways, reaction sequences that build up the complexity of biomolecules, remains rare. The anabolic pathways of greatest interest for proto-anabolism are specific reductive  $\text{CO}_2$ -fixing pathways used by chemoautotrophs;<sup>14</sup> the AcCoA (Wood-Ljungdahl) pathway,<sup>5–9,15</sup> complete or incomplete versions of the reductive tricarboxylic acid (rTCA or reductive Krebs) cycle,<sup>16–19</sup> or hypothetical combinations thereof.<sup>20,21</sup> These synthetic pathways are proposed to have been spontaneously driven into existence as a mechanism to dissipate geochemical redox gradients built up between the Earth's reduced core (mostly  $\text{Fe}^0$ ) and its relatively oxidized atmosphere,<sup>22</sup> providing an origins scenario that is continuous from geochemistry to the reductive thermophilic carbon-fixing organisms found at the root of the tree of life.<sup>19,23,24</sup> The rTCA cycle exhibits further appeal as a prebiotic pathway since it contains all five universal metabolic precursors for biosynthesis, consists of only five mechanistically distinct reactions, does not use bimolecular reactions between intermediates, and possesses an autocatalytic feedback loop that could allow it to persist and self-amplify under the right conditions.<sup>18,25</sup> Hypothetical proto-anabolic networks consisting of the AcCoA pathway together with the complete rTCA cycle,<sup>20</sup> or the AcCoA pathway together with an incomplete linear version of the rTCA that stops after step F (Figure 1),<sup>6,21</sup> have also been suggested as primordial synthetic pathways. The “complete” hybrid pathway constitutes a stabilized autocatalytic network that, once realized, could display robustness in the face of low synthetic efficiencies or parasitic reactions, providing a compelling reason for why its molecules were preserved in metabolism. On the other hand, an incomplete linear hybrid network is shorter and more plausible under non-enzymatic catalysis due to the challenge of diminishing yields faced in any sequence of chemical reactions.<sup>26</sup>

The reductive coupling of two molecules of  $\text{CO}_2$  to acetate (**1**), equivalent to the AcCoA pathway, has been observed under aqueous conditions either by using  $\text{Fe}^0$  nanoparticles as reducing agents or through electrochemistry on greigite electrodes, albeit in small quantities and with poor selectivity.<sup>27–29</sup> Acetate production from CO and MeSH in the presence of (Fe,Ni)S has also been reported.<sup>30</sup> Experimental efforts to test the plausibility of a prebiotic rTCA cycle have not been as encouraging.<sup>31,32</sup> Thus far, only two non-consecutive steps of the rTCA cycle (steps C and E, Figure 1) have been reported with >5% yield under plausibly prebiotic conditions by using mineral photocatalysis.<sup>32</sup> Notably, pyruvate has been observed in low yields under electrochemical<sup>28</sup> and CO-rich hydrothermal conditions.<sup>33</sup> Further efforts are needed to test the plausibility of an abiotic (complete or incomplete) rTCA cycle which, when viewed together with an abiotic AcCoA pathway, would provide a satisfying theory for the origin and organization of modern biochemistry. Herein we describe our efforts to assess the prebiotic viability of the six reduction and (de)hydration steps of the rTCA cycle under the influence of metals and metal ions.<sup>34</sup>

## Results and discussion

Of initial consideration was a search for a viable reducing agent for the two ketone reductions (steps C and H) and one alkene reduction (step E). In biological systems, steps C and H use NADPH as reducing agent and are catalyzed by malate dehydrogenase and isocitrate dehydrogenase, respectively; step E uses FADH as reducing agent and is catalyzed by fumarate reductase. The ketone reductions are thought to be challenging as prebiotic processes due to the rapid spontaneous decarboxylation of oxaloacetate **3** and oxalosuccinate **8**.<sup>35</sup> In aqueous solution, **3** has indeed only been observed to be reduced photochemically.<sup>32</sup> A preliminary screen of simple chemical reducing agents ( $\text{Fe}^0$ ,  $\text{Ni}^0$ ,  $\text{Zn}^0$ ,  $\text{Mn}^0$ ,  $\text{Mo}^0$ ,  $\text{Na}_2\text{S}_2\text{O}_4$ ) at various temperatures and across pH ranges revealed several that were capable of some or all of the reductions, but  $\text{Fe}^0$  under acidic aqueous conditions stood out for its unique ability to accomplish all three desired individual reductions (Table 1, entries 1-3) while minimizing undesired parasitic reactions and promoting sequences (*vide infra*). These observations, in addition to the geological relevance of iron as the major constituent of the Earth's core and the widespread occurrence of its salts in native element minerals, prompted us to select  $\text{Fe}^0$  as reducing agent for further experiments.

In biological systems, the dehydrations of malate **4** to fumarate **5** and of isocitrate **9** to *cis*-aconitate **10** (steps D and I) are carried out by the enzymes malate dehydratase and aconitase, respectively. We surmised that these steps should be particularly prone to metal ion catalysis since some dehydratases are  $\text{Fe}^{2+}$ -dependent and since aconitase makes use of a Lewis acidic Fe-S cluster to facilitate isocitrate dehydration.<sup>36</sup> The dehydrations of **4** and **9** are both slightly endergonic (+2.3 kJ/mol) at neutral pH.<sup>18</sup> Perhaps not surprisingly given these unfavorable thermodynamics, in both cases no more than trace dehydration products were detected upon heating to 140 °C in acidic or basic solution, even in the presence of a wide selection of metal ions. In contrast, the thermodynamically favored hydration of **5** to **4** occurs even in the absence of metal ions (entry 4). We therefore sought to push the dehydration forward by coupling the small amounts of **5** generated at chemical equilibrium to the subsequent irreversible reduction step (D-E). A screen of various metal ions in the presence of  $\text{Fe}^0$  revealed that  $\text{Zn}^{2+}$  ions in acidic solution at 140 °C were effective to mediate the dehydration of **4** to **5** and putative reduction to **6** in a single operation, albeit in low yield (entry 5; see also Supplementary Table 2). We next carried out the same reaction in the presence of a 1% w/w aqueous micellar solution of  $\alpha$ -tocopherol methoxypolyethylene glycol succinate, a popular non-ionic surfactant that self-assembles into nano-sized reaction compartments,<sup>37</sup> and found that it promoted the two-step sequence even at ambient temperature (entry 6). Though this micelle has no direct prebiotic relevance, the experiment supports existing ideas that compartmentalization can enhance the efficiency of prebiotic metabolic processes.<sup>1</sup> A similar screen of metal ions at various temperatures and pH values revealed the dehydration of **9** to **10** to also be promoted by  $\text{Zn}^{2+}$  ions under hot acidic aqueous conditions (entry 7; see also Supplementary Table 3). Like the enzymatic system, step I is reversible under these conditions (entry 8).

The sole hydration reaction of the rTCA cycle is the hydration of *cis*-aconitate **10** to citrate **11** (step J), a reaction that is also carried out in biological systems by the FeS cluster enzyme aconitase. All attempts to observe this reaction under simple acid or base catalysis failed. To

our delight, a screen of more than 20 different metal ions at various temperatures and pH values revealed that  $\text{Cr}^{3+}$  was uniquely effective at enabling hydration to yield substantial amounts of citrate in acidic solution at 140 °C (entry 9).<sup>38</sup> Much smaller amounts of citrate were observed in the presence of other metal ions or at lower temperatures (Supplementary Table 4). Again, like the enzymatic system, step J was found to be reversible under these conditions (entry 10). The observation that  $\text{Zn}^{2+}$  and  $\text{Cr}^{3+}$  promote hydration and dehydration only under acidic conditions can be ascribed to the tendency of metal cations to become aquated at low pH, where they may form structurally diverse polynuclear species that can complex the rTCA acids. In contrast, under alkaline aqueous conditions many transition metal ions form hydroxides that do not efficiently bind carboxylic acids. In analogy to prior studies on metal ion promoted hydration,<sup>38</sup> we propose that upon binding of the carboxylic acid to the aquated metal ion, the dehydration (Figure 3a) or hydration (Figure 3b) occurs with the assistance of water molecules present in the second coordination sphere of the metal complex. This proposed mechanism is also similar to the well-studied mechanism of enzymatic hydration/dehydration catalyzed by aconitase, in the sense that  $\text{Zn}^{2+}$  performs the function of the FeS cluster's "isocitrate mode" and  $\text{Cr}^{3+}$  performs the function of its "citrate mode".<sup>39</sup>

The realization that various combinations of  $\text{Fe}^0$ ,  $\text{Zn}^{2+}$ ,  $\text{Cr}^{3+}$  and micelles can mediate the individual reduction, dehydration and hydration reactions of the rTCA cycle prompted us to assess their mutual compatibility for three-step reduction/(de)hydration sequences. The reduction/dehydration/reduction sequence starting from oxaloacetate **3** (steps C,D,E) works in the presence of all promoting components to deliver **6** even at ambient temperature (entry 11; see Supplementary Table 1 for control experiments). Next, we evaluated the three-step reduction/dehydration/hydration sequence spanning steps H, I and J. Heating an acidic aqueous solution containing **8**,  $\text{Fe}^0$ ,  $\text{Zn}^{2+}$  and  $\text{Cr}^{3+}$  to 140 °C indeed resulted in the formation of **11** (entry 12). The presence of micelles had little effect on the outcome of this sequence (entry 13). These results demonstrate that sequences of non-enzymatic reactions of the rTCA cycle are possible with the help of simple, mutually compatible reagents.

A notable criticism by Orgel concerning the hypothesis of a prebiotic complete rTCA cycle is the difficulty for simple non-enzymatic catalysts to promote the reactions of the cycle over parasitic reactions with sufficient selectivity to achieve the theoretical 50% efficiency threshold such that autocatalysis could self-sustain or self-amplify.<sup>26</sup> Although this criticism does not take into account the possibility that the rTCA cycle might be sustained at lower efficiency thresholds with the help of feeder pathways such as the AcCoA pathway,<sup>20</sup> it nonetheless correctly points out that *on-cycle vs off-cycle* selectivity imposes important kinetic constraints on the sustainability of an autocatalytic reaction network. We therefore set out to assess the level of selectivity for *on-cycle* (steps C, E and H) over *off-cycle* reduction reactions (mauve arrows, Figure 2). Several potential "dead-end" reduction reactions may lead off-cycle, such as the reduction of **2** to give lactate **12**, the reduction of **7** to give  $\alpha$ -hydroxyglutarate **13** and the reduction of **10** to give tricarballoylate **14**. A competitive reduction experiment on a mixture of five rTCA cycle intermediates (**2**, **3**, **5**, **7**, **10**) in the presence of all identified reaction promoters (10 equiv  $\text{Fe}^0$ ,  $\text{Zn}^{2+}$ ,  $\text{Cr}^{3+}$ , micelles) revealed that <5% of the compounds observed in the mixture after 3 h at 40 °C were derived

from *off-cycle* reduction (entry 14). Notably, a similar competitive reduction experiment using  $\text{Ni}^0$  as the reducing agent gave even higher levels of selectivity, but  $\text{Ni}^0$  was less effective at promoting reaction sequences (Supplementary Tables 5 and 7). Since the most sensitive compounds, such as **3** and **8**, are both reduced at temperatures below 40 °C, the survival of a complete reaction network shown in Figure 1 may be feasible in the presence of  $\text{Zn}^{2+}$  and  $\text{Cr}^{3+}$  in a reaction environment that cycles over a temperature gradient of approximately 20-140 °C and where **3** and **8** are produced and reduced at the cooler end of that temperature range. It is not clear whether or not such thermal cycling could be achieved in a natural environment under acidic conditions. However, since steps C-E all occur at 20 °C in the presence of  $\text{Zn}^{2+}$  and micelles, the observed selectivity is also compatible with a linear reaction network incorporating the AcCoA pathway and an incomplete rTCA cycle that stops after step F, without invoking thermal cycling.<sup>6,21</sup>

A crucial aspect of any prebiotic reaction network is the ability to branch out into productive synthetic pathways that might eventually contribute to the stability of the network. We therefore became interested in the production of  $\alpha$ -amino acids by reductive amination of the  $\alpha$ -ketoacids of the rTCA cycle, in analogy with biosynthesis (Figure 2, light blue arrow). Although reductive amination of  $\alpha$ -ketoacids with  $\text{NH}_3$  in aqueous solution is known,<sup>40,41</sup> it is challenging under the highly acidic conditions required for metal ion promotion of the rTCA cycle since all  $\text{NH}_3$  is trapped as  $\text{NH}_4^+$ . We speculated that  $\text{NH}_2\text{NH}_2$ , which is an intermediate and product of biological and abiological  $\text{N}_2$  reduction,<sup>42,43</sup> could be an effective surrogate for  $\text{NH}_3$  under acidic conditions, since it should retain one free amino group and thus remain available for reaction with  $\alpha$ -ketoacids. The initial product of reductive amination of the  $\alpha$ -ketoacid with hydrazine is presumably a hydrazone, which possesses a weak N-N bond and which we suspected could be subsequently cleaved under the same reducing conditions to yield amino acids (Figure 3c). Indeed, exposure of **2** to just 2 equiv of  $\text{NH}_2\text{NH}_2$  and excess  $\text{Fe}^0$  under typical acidic conditions at 80 °C resulted in the formation of alanine **15** as the major product (entry 15). This reactivity was maintained with  $\text{Fe}^0$  across a wide temperature range (25 – 140 °C), while the use of  $\text{Ni}^0$  as reducing agent furnished alanine only at 140 °C (Supplementary Table 6). The requisite amount of  $\text{NH}_2\text{NH}_2$  is notably far less than the >100-fold excess of  $\text{NH}_3$  required in other reductive aminations under aqueous conditions,<sup>40</sup> allowing reduced nitrogen to be viewed as a limiting feedstock for prebiotic chemistry, rather than one required in large excess.

## Conclusion

We have demonstrated that more than half of the rTCA cycle, an anabolic pathway central to biochemistry, can be promoted under a common set of conditions by just two metal ions and driven by  $\text{Fe}^0$  with *on-cycle* selectivity, a feat normally carried out by the action of five different enzymes. Amino acid synthesis via reductive amination using  $\text{Fe}^0$  and  $\text{NH}_2\text{NH}_2$  also occurs under the typical conditions. These observations bolster the plausibility of a non-enzymatic rTCA cycle or an incomplete variant thereof as a prebiotic pathway and should be taken into account in future attempts to model prebiotic metabolism.<sup>44</sup> They also demonstrate that metal ions such as  $\text{Zn}^{2+}$  and  $\text{Cr}^{3+}$  can promote reactions typically associated with Fe-S cluster enzymes. Indeed, several authors have argued for an important role for  $\text{Zn}^{2+}$  in prebiotic chemistry or early life.<sup>45,46</sup> The conditions described here are

remarkably similar to those reported for the generation of acetate from CO<sub>2</sub> and Fe<sup>0</sup> nanoparticles,<sup>27</sup> providing hope that a prebiotic reaction network containing both the AcCoA pathway and (at least parts of) the rTCA cycle may eventually be identified. The acidic conditions identified for metal ion promotion of the rTCA cycle seem more compatible with acidic or locally acidic metal-rich environments such as those found in some hydrothermal fields and hydrothermal vents.<sup>47,48</sup> This is in agreement with previous observations of enhanced stability of peptide, RNA phosphodiester and aminoacyl-(t)RNA bonds at acidic pH.<sup>49</sup> Although Fe<sup>0</sup> and Ni<sup>0</sup> are themselves generally considered to be rare near the Earth's surface, we note that electric currents with negative potentials have recently been observed across the surfaces of acidic hydrothermal vents.<sup>50</sup> An electric current with a potential between those of Fe<sup>0</sup> and Ni<sup>0</sup> could provide a continuous supply of electrons with similar reactivity and selectivity to that observed in our study. Ongoing investigations in our laboratories are focused on identifying catalysts and conditions for the C-C bond-forming reactions of the rTCA cycle and the AcCoA pathway, as well as interfacing with other productive *off-cycle* anabolic pathways including gluconeogenesis.

## Methods

### Analytical methods

GC-MS analysis was performed on a GC System 7820A (G4320) connected to a MSD block 5977E (G7036A), using Agilent High Resolution Gas Chromatography Column: PN 19091S – 433UI, HP – 5MS UI, 28 m×0.250 mm, 0.25 Micron, SN USD 489634H. All samples were prepared in ethyl acetate (200 µL sample volume). The analysis was carried out on a splitless 1 µL injection volume with an injection port temperature 250 °C. Column oven temperature program was as follows: 60 °C for 1 min, ramped at 30 °C min<sup>-1</sup> to 310 °C with 3 min hold, with a total running time of 12.33 min. The mass spectrometer was turned on after 2 min and was operated at the electron ionization mode with quadrupole temperature of 150 °C. Data acquisition was performed in the full-scan mode (50-500). Hydrogen (99.999 % purity) was used as carrier gas at a constant flow rate of 1.5 mL min<sup>-1</sup>.

### Derivatization and Product Identification

For optimal gas chromatography resolution, carboxylic acids used in this study were converted to ethyl esters using a mixture of ethanol/ethyl chloroformate (EtOH/ECF) or to methyl esters using a mixture of methanol/methyl chloroformate (MeOH/MCF), as described in the Supplementary Information. Reaction products were identified by comparing the mass spectra and retention times of derivatized authentic samples (Supplementary Figures 1-15) against analogously derivatized samples obtained from the reaction (Supplementary Figures 16-54). ECF derivatization was preferred for small molecule substrates (pyruvate, lactate, malate, fumarate, succinate, α-ketoglutarate and α-hydroxyglutarate, alanine), while MCF derivatization gave clearer results (less elimination by-products and better resolution) for *cis*-aconitate, tricarballoylate, isocitrate and citrate.

### Quantification and error analysis

For the purposes of this study, reported are not the absolute percentage yields based on the number of moles of the starting materials, but rather percentage contributions to the total

composition of the final reaction mixture. This allows to account for potential concentration changes due to solvent loss (since many reactions were carried out in sealed tubes at temperatures above the boiling point of water), as well as potentially incomplete extraction during the derivatization procedure. The compound distributions were calculated by comparing the product peak area with the GC-MS calibration lines (Supplementary Figures 55-67). Each reaction was performed at least twice and reported percentage compositions are an average of these runs. Mean absolute deviations associated with the mean values shown in Table 1 can be found in Supplementary Table 1.

### General procedure for Fe<sup>0</sup>/ Zn<sup>2+</sup>/Cr<sup>3+</sup> and Ni<sup>0</sup>/Zn<sup>2+</sup>/Cr<sup>3+</sup> promoted reactions

To a 10 mL Pyrex pressure tube containing a Teflon-coated magnetic stir bar was added (unless otherwise specified) carboxylic acid substrate(s) (1 equiv, 0.100 mmol of each acid), Fe<sup>0</sup> or Ni<sup>0</sup> powder (10 equiv, 1.0 mmol, 56 mg Fe<sup>0</sup> or 59 mg Ni<sup>0</sup>), and/or ZnCl<sub>2</sub> (15 equiv, 1.50 mmol, 204 mg), and/or Cr<sub>2</sub>(SO<sub>4</sub>)<sub>3</sub>·12H<sub>2</sub>O (3 equiv, 0.300 mmol, 183 mg). This was followed by the addition of 3 mL of solvent (unless otherwise specified: 1 M HCl in H<sub>2</sub>O). The contents of the tube were flushed with argon for ≈ 30 s. The tube was then quickly sealed and the reaction mixture magnetically stirred for 16 h in a 12-tube metal heating block that was maintained at an internal temperature of 140 °C using an electronic thermocouple. The reaction tube was then removed from the heating block and allowed to cool to room temperature prior to derivatization and GC-MS analysis.

### General procedure for reductive amination

A solution of sodium pyruvate (1 equiv, 0.100 mmol, 11.0 mg) and Cr<sub>2</sub>(SO<sub>4</sub>)<sub>3</sub>·12H<sub>2</sub>O (3 equiv, 0.300 mmol, 183 mg) in 1 M HCl in H<sub>2</sub>O (3 mL) was added to a 10 mL Pyrex pressure tube containing a Teflon-coated magnetic stir bar. Hydrazine monohydrate (2 equiv, 0.20 mmol, ~10 μL) was then added, followed by Fe<sup>0</sup> or Ni<sup>0</sup> powder (10 equiv, 1.0 mmol, 56 mg Fe<sup>0</sup> or 59 mg Ni<sup>0</sup>). The tube was then quickly sealed and the reaction mixture magnetically stirred for 16 h in a 12-tube metal heating block that was maintained at the specified internal temperature (20-140 °C) using an electronic thermocouple. The reaction tube was then removed from the heating block and allowed to cool to room temperature prior to derivatization and GC-MS analysis.

**Metal screens for malate dehydration**—Inorganic salts containing the following metals were used in the reaction screen: Zn<sup>2+</sup>, Cu<sup>2+</sup>, Ni<sup>2+</sup>, Co<sup>2+</sup>, Fe<sup>2+</sup>, Mn<sup>2+</sup>, Cr<sup>2+</sup>, V<sup>2+</sup>. Zn<sup>2+</sup> gave the best yields when used together with Fe<sup>0</sup> (2-step reaction). For detailed metal screens see Supplementary Table 2.

**Metal screens for isocitrate dehydration**—Inorganic salts containing the following metals were used in the reaction screen: Zn<sup>2+</sup>, Cu<sup>2+</sup>, Ni<sup>2+</sup>, Co<sup>2+</sup>, Fe<sup>2+</sup>, Mn<sup>2+</sup>, Cr<sup>2+</sup>, V<sup>2+</sup>, Pd<sup>2+</sup>, Cd<sup>2+</sup>, Fe<sup>3+</sup>, Mn<sup>3+</sup>, Cr<sup>3+</sup>, As<sup>3+</sup>, Ru<sup>3+</sup>, Ir<sup>3+</sup>, Rh<sup>3+</sup>, Ti<sup>3+</sup>. Zn<sup>2+</sup> was selected for further experiments due to high yields and geochemical accessibility, although substantial reactivity was also observed for Cr<sup>2+</sup>, Pd<sup>2+</sup>, Fe<sup>3+</sup>, Mn<sup>3+</sup>, As<sup>3+</sup>, Ru<sup>3+</sup>, Ir<sup>3+</sup> and Rh<sup>3+</sup>. For detailed metal screens see Supplementary Table 3.

**Metal screens for aconitate hydration**—Inorganic salts containing the following metals were used in the reaction screen:  $\text{Cu}^+$ ,  $\text{Zn}^{2+}$ ,  $\text{Cu}^{2+}$ ,  $\text{Ni}^{2+}$ ,  $\text{Co}^{2+}$ ,  $\text{Fe}^{2+}$ ,  $\text{Mn}^{2+}$ ,  $\text{Cr}^{2+}$ ,  $\text{Cd}^{2+}$ ,  $\text{Hg}^{2+}$ ,  $\text{Fe}^{3+}$ ,  $\text{Co}^{3+}$ ,  $\text{Mn}^{3+}$ ,  $\text{Cr}^{3+}$ ,  $\text{Ti}^{3+}$ ,  $\text{Ru}^{3+}$ ,  $\text{Mo}^{4+}$ ,  $\text{W}^{4+}$ ,  $\text{Mo}^{6+}$ ,  $\text{W}^{6+}$ . Only  $\text{Cr}^{3+}$  returned a substantial positive result. For detailed metal screens see Supplementary Table 4.

## Supplementary Material

Refer to Web version on PubMed Central for supplementary material.

## Acknowledgements

This project has received funding from the European Research Council (ERC) under the European Union's Horizon 2020 research and innovation program (grant agreement n° 639170). Further funding was provided by a grant from LabEx “Chemistry of Complex Systems”. We thank the ELSI Origins Network (EON), which is supported by a grant from the John Templeton Foundation and provided through the Earth-Life Science Institute of the Tokyo Institute of Technology. Prof. Eric Smith is thanked for stimulating discussions. This paper is dedicated to the memory of Prof. Harold J. Morowitz.

## References

- (1). Ruiz-Mirazo K, Briones C, de la Escosura A. Prebiotic Systems Chemistry: New Perspectives for the Origins of Life. *Chem Rev.* 2014; 114:285–366. [PubMed: 24171674]
- (2). Peretó J. Out of fuzzy chemistry: from prebiotic chemistry to metabolic networks. *Chem Soc Rev.* 2012; 41:5394–5403. [PubMed: 22508108]
- (3). Sutherland JD. Studies on the origin of life—the end of the beginning. *Nat Rev Chem.* 2017; 1:1.
- (4). Morowitz, HJ. *Beginnings of Cellular Life: Metabolism Recapitulates Biogenesis.* Yale Univ Press; 1992.
- (5). Wächtershäuser G. Before enzymes and templates: theory of surface metabolism. *Microbiol Rev.* 1988; 52:452–484. [PubMed: 3070320]
- (6). Martin W, Russell MJ. On the origin of biochemistry at an alkaline hydrothermal vent. *Phil Trans R Soc B.* 2007; 362:1887–1926. [PubMed: 17255002]
- (7). Peretó JG, Velasco AM, Becerra A, Lazcano A. Comparative biochemistry of  $\text{CO}_2$  fixation and the evolution of autotrophy. *Int Microbiol.* 1999; 2:3–10. [PubMed: 10943384]
- (8). Lane N, Allen JF, Martin W. How did LUCA make a living? Chemiosmosis in the origin of life. *Bioessays.* 2010; 32:271–280. [PubMed: 20108228]
- (9). Russell MJ, Nitschke W, Branscomb E. The inevitable journey to being. *Phil Trans R Soc B.* 2013; 368 20120254.
- (10). Sutherland JD. The Origin of Life—Out of the Blue. *Angew Chem Int Ed.* 2015; 55:104–121.
- (11). Keller MA, Turchyn AV, Ralser M. Non-enzymatic glycolysis and pentose phosphate pathway-like reactions in a plausible Archean ocean. *Mol Syst Biol.* 2014; 10:725. [PubMed: 24771084]
- (12). Keller, et al. Conditional iron and pH-dependent activity of a non-enzymatic glycolysis and pentose phosphate pathway. *Sci Advances.* 2016; 2:e1501235. [PubMed: 26824074]
- (13). Keller MA, Kampjut D, Harrison SA, Ralser M. Sulfate radicals enable a non-enzymatic Krebs cycle precursor. *Nat Eco Evo.* 2017; 1:0083.
- (14). Berg, et al. Autotrophic carbon fixation in archaea. *Nat Rev Microbiol.* 2010; 8:447–460. [PubMed: 20453874]
- (15). Ljungdahl LG, Irion E, Wood HG. Total synthesis of acetate from  $\text{CO}_2$ . I. Co-methylcobyrinic acid and Co-(methyl)-5-methoxy-benzimidizolycobamide as intermediates with *Clostridium thermoaceticum*. *Biochemistry.* 1965; 4:2771–2779. [PubMed: 5880685]
- (16). Evans MCW, Buchanan BB, Arnon DI. A New Ferredoxin-Dependent Carbon Reduction Cycle in a Photosynthetic Bacterium. *P Natl Acad Sci.* 1966; 55:928–934.
- (17). Morowitz HJ, Kostelnik JD, Yang J, Cody GD. The origin of intermediary metabolism. *P Natl Acad Sci.* 2000; 97:7704–7708.



- (18). Smith E, Morowitz HJ. Universality in intermediary metabolism. *P Natl Acad Sci.* 2004; 101:13168–13173.
- (19). Smith, E., Morowitz, HJ. *The Origin and Nature of Life on Earth: The Emergence of the Fourth Geosphere.* Cambridge Univ Press; 2016.
- (20). Braakman R, Smith E. The emergence and early evolution of biological carbon-fixation. *PLoS Comp Biol.* 2012; 8:e1002455.
- (21). Camprubi E, Jordan SF, Vasiliadou R, Lane N. Iron catalysis at the origin of life. *IUBMB Life.* 2017; 69:373–381. [PubMed: 28470848]
- (22). Russell, MJ., Hall, AJ., Mellersh, AR. *On the Dissipation of Thermal and Chemical Energies on the Early Earth. Natural and Laboratory-Simulated Thermal Geochemical Processes.* Springer Netherlands; 2003.
- (23). Reysenbach A-L, Shock E. Merging genomes with geochemistry in hydrothermal ecosystems. *Science.* 2002; 296:1077–1082. [PubMed: 12004120]
- (24). Weiss, et al. The physiology and habitat of the last universal common ancestor. *Nat Microbiol.* 2016; 1:16116. [PubMed: 27562259]
- (25). Plasson R, Brandenburg A, Jullien L, Bersini H. Autocatalyses. *J Phys Chem A.* 2011; 115:8073–8085. [PubMed: 21650179]
- (26). Orgel LE. The implausibility of metabolic cycles on the prebiotic earth. *PLoS Biol.* 2008; 6:e18. [PubMed: 18215113]
- (27). He C, Tian G, Liu Z, Feng S. A mild hydrothermal route to fix carbon dioxide to simple carboxylic acids. *Org Lett.* 2010; 12(4):649. [PubMed: 20104858]
- (28). Roldan A, Hollingsworth N, Roffey A, Islam H-U, Goodall JBM, Catlow CRA, Darr JA, Bras W, Sankar G, Holt KB, Hogarth G, et al. Bio-inspired CO<sub>2</sub> conversion by iron sulfide catalysts under sustainable conditions. *Chem Commun.* 2015; 51:7501.
- (29). Herschy B, Whicher A, Camprubi E, Watson C, Dartnell L, Ward J, Evans JRG, Lane N. An Origin-of-Life Reactor to Simulate Alkaline Hydrothermal Vents. *Journal of Molecular Evolution.* 2014; 79:213–227. [PubMed: 25428684]
- (30). Huber C, Wächtershauser G. Activated acetic acid by carbon fixation on (Fe,Ni)S under primordial conditions. *Science.* 1997; 276:245–247. [PubMed: 9092471]
- (31). Cody GD, et al. Geochemical roots of autotrophic carbon fixation: hydrothermal experiments in the system citric acid, H<sub>2</sub>O-(±FeS)-(±NiS). *Geochemica et Cosmochemica Acta.* 2001; 65:3557–3576.
- (32). Zhang XV, Martin ST. Driving parts of Krebs cycle in reverse through mineral photochemistry. *J Am Chem Soc.* 2006; 128:16032–16033. [PubMed: 17165745]
- (33). Cody GD, et al. Primordial carbonylated iron-sulfur compounds and the synthesis of pyruvate. *Science.* 2000; 289:1337–1340. [PubMed: 10958777]
- (34). Morowitz HJ, Srinivasan V, Smith E. Ligand field theory and the origin of life as an emergent feature of the periodic table of elements. *Biol Bull.* 2010; 219:1–6. [PubMed: 20813983]
- (35). Ross DS. The viability of a nonenzymatic reductive citric acid cycle – kinetics and thermochemistry. *Orig Life Evol Biosphere.* 2007; 37:61–65.
- (36). Flint DH, Allen RM. Iron–sulfur proteins with nonredox functions. *Chem Rev.* 1996; 96:2315–2334. [PubMed: 11848829]
- (37). Lipshutz BH, Ghorai S, Abela AR, Moser R, Nishikata T, Duplais C, Krasovskiy A, Gaston RD, Gadwood RC. TPGS-750-M: A Second-Generation Amphiphile for Metal-Catalyzed Cross-Couplings in Water at Room Temperature. *J Am Chem Soc.* 2011; 76:4379–4391.
- (38). Olson MV, Taube H. Hydration and isomerization of coordinated maleate. *J Am Chem Soc.* 1970; 92:3236–3237.
- (39). Nicolet, Y., Fontecilla-Camps, JC. Fe–S Clusters: Biogenesis and Redox, Catalytic, and Regulatory Properties, in *Bioinspired Catalysis.* Wiley-VCH Verlag GmbH & Co. KGaA; Weinheim, Germany; 2014.
- (40). Huber C, Wächtershäuser G. Primordial reductive amination revisited. *Tetrahedron Lett.* 2003; 44:1695–1697.

- (41). Wang W, et al. Photocatalytic reversible amination of  $\alpha$ -keto acids on a ZnS surface: implications for the prebiotic metabolism. *Chem Commun.* 2012; 48:2146.
- (42). Dietl A, et al. The inner workings of the hydrazine synthase multiprotein complex. *Nature.* 2015; 527:394–297. [PubMed: 26479033]
- (43). Barney BM, Laryukhin M, Igarashi RY, Lee HI, Dos Santos PC, Yang TC, Hoffman BM, Dean DR, Seefeldt LC. *Biochemistry.* 2005; 44:8030–8037. [PubMed: 15924422]
- (44). Zubarev DY, Rappoport D, Aspuru-Guzik A. Uncertainty of prebiotic scenarios: the case of the non-enzymatic reverse tricarboxylic acid cycle. *Sci Rep.* 2015; 5:8009. [PubMed: 25620471]
- (45). Zerkle AL, House CH, Brantley SL. Biogeochemical signatures through time as inferred from whole microbial genomes. *Am J Sci.* 2005; 305:467–502.
- (46). Mulkidjanian AY, Galperin MY. On the origin of life in the zinc world. 2. Validation of the hypothesis on the photosynthesizing zinc sulfide edifices as cradles of life on Earth. *Biol Direct.* 2009; 4:27. [PubMed: 19703275]
- (47). Martin W, Baross J, Kelley D, Russell MJ. Hydrothermal vents and the origin of life. *Nat Rev Microbiol.* 2008; 6:805–814. [PubMed: 18820700]
- (48). Ross DS, Deamer D. Dry/Wet Cycling and the Thermodynamics and Kinetics of Prebiotic Polymer Synthesis. *Life.* 2016; 6:28.
- (49). Bernhardt HS, Tate WP. Primordial soup or vinaigrette: did the RNA world evolve at acidic pH? *Biol Direct.* 2012; 7:4. [PubMed: 22264281]
- (50). Nakamura R, et al. Electrical Current Generation across a Black Smoker Chimney. *Angew Chem Int Ed.* 2010; 49:7692.

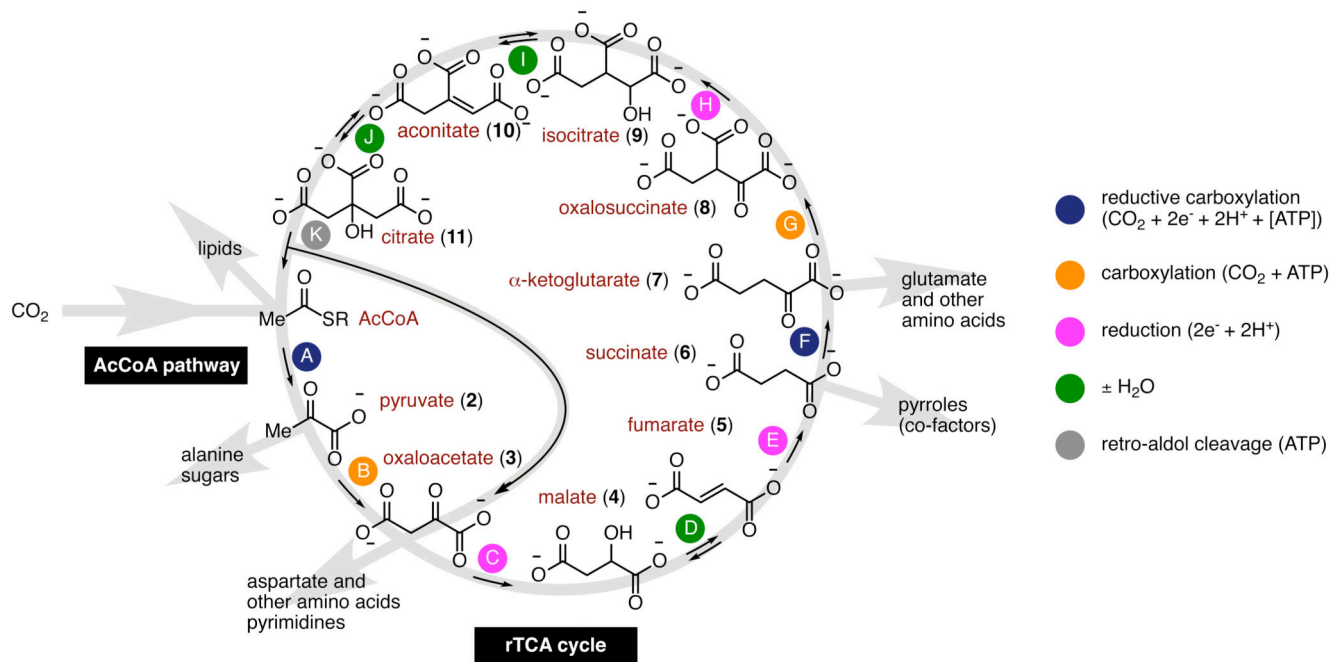


**Figure 1.** Hypothetical proto-anabolic network consisting of the AcCoA pathway (CO<sub>2</sub> to AcCoA) and the rTCA cycle, including the epicycle for oxaloacetate synthesis, showing the role of its intermediates as universal biosynthetic precursors (ref. 19, 20). Variants with an incomplete rTCA cycle that stops after step F have also been proposed (refs. 6, 21).

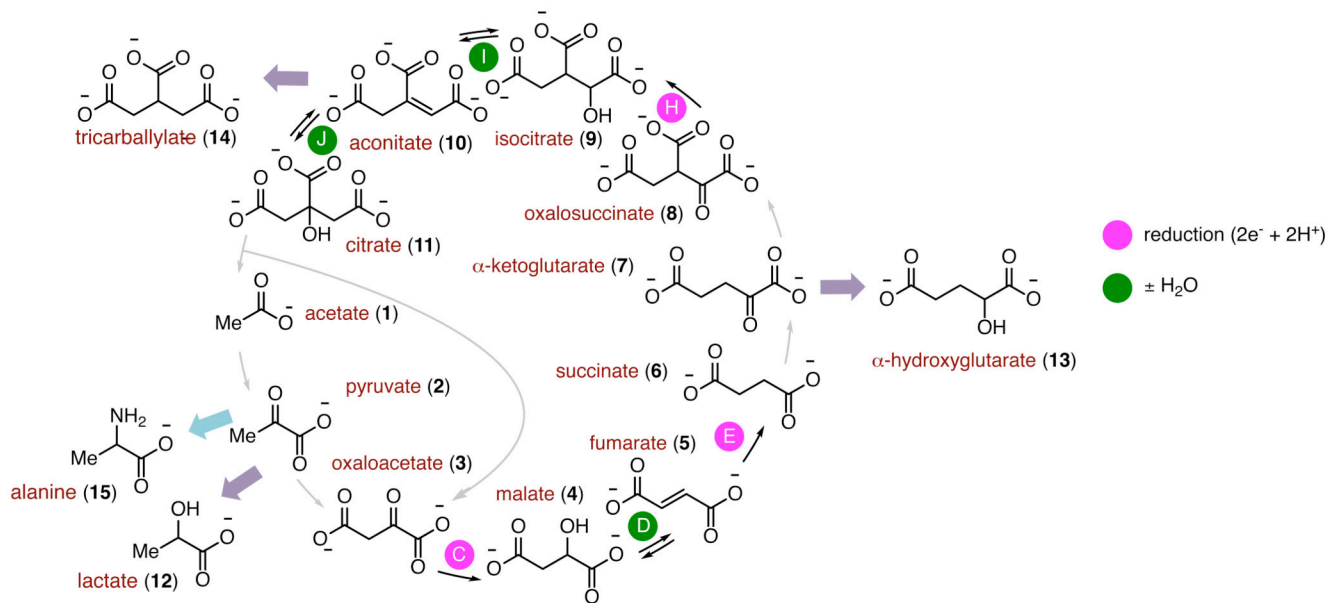


**Figure 2.** Prebiotic reaction network showing the rTCA cycle, reductive amination (light blue arrow) and potential off-cycle reductions (mauve arrows). For consistency with Figure 1, compounds are drawn in their anionic form, however under the acidic experimental conditions the compounds exist in their protonated form.

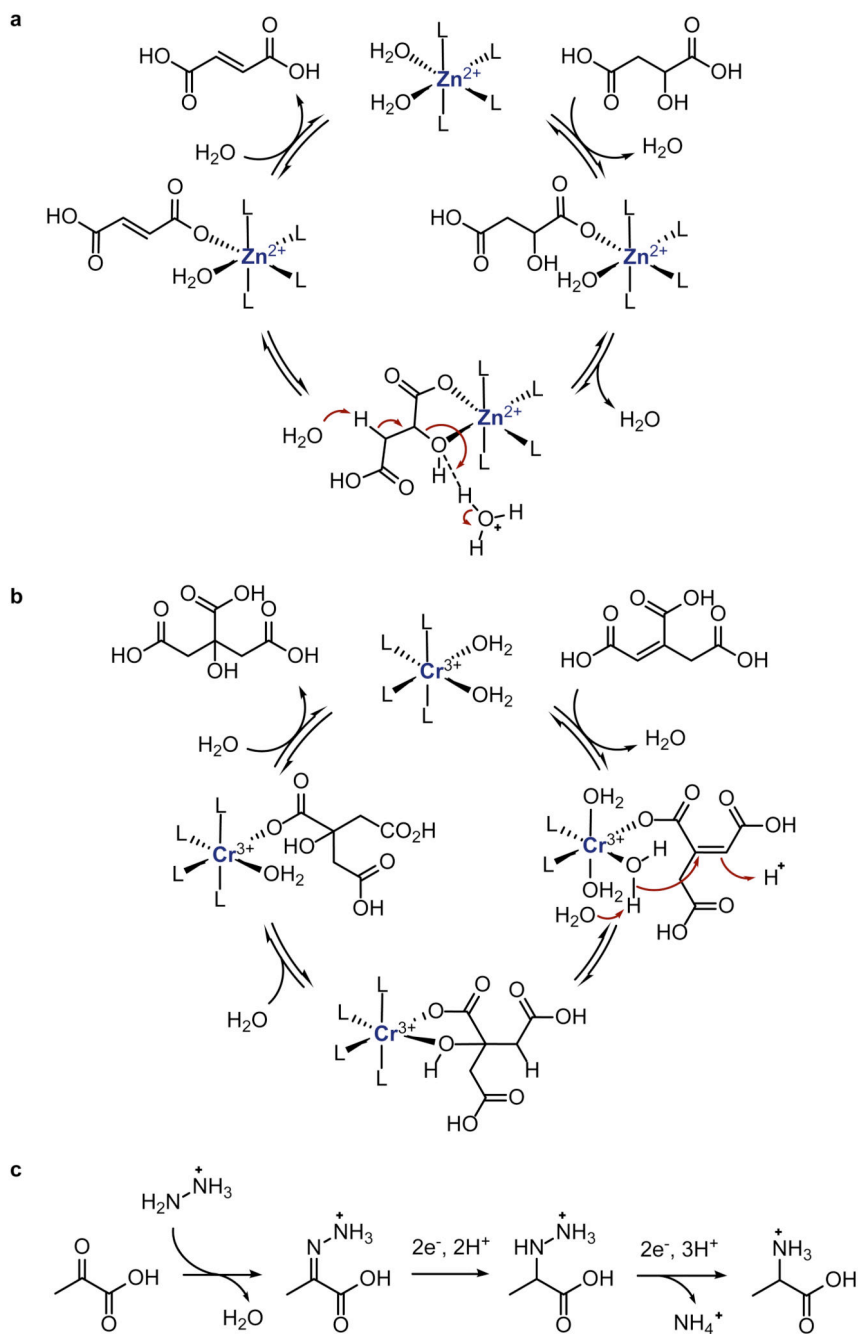


**Figure 3.** Plausible chemical mechanisms of a) reversible Zn<sup>2+</sup> promoted dehydration of malate or isocitrate; b) reversible Cr<sup>3+</sup> promoted hydration of aconitate; c) reductive amination of pyruvate with hydrazine and subsequent reductive N-N bond cleavage to generate alanine. Metal complexes are depicted as mononuclear species for clarity. L = undefined ligand.

**Table 1**  
**Non-enzymatic reactions of the rTCA cycle.**

Entry	Substrate (0.1 mmol)	Conditions <sup>a</sup>				Species detected in the mixture post-reaction (%) <sup>‡</sup>										
		Fe <sup>0</sup> (equiv.)	Zn <sup>2+</sup> (equiv.)	Cr <sup>3+</sup> (equiv.)	Micelles	On-cycle										Off-cycle
		2	4	5	6	7	9	10	11	12	13	14	15			
<i>Reduction</i>																
1	3	10	-	-	-	90	10									
2 <sup>b</sup>	5	10	-	-	-	15	20	65								
3 <sup>c</sup>	8	10	-	-	-			2	98							
<i>Hydration/Dehydration</i>																
4 <sup>d</sup>	5	-	-	-	-	77	23									
5 <sup>d</sup>	4	10	10	-	-	94	4	2								
6 <sup>e</sup>	4	10	10	-	yes	82	7	11								
7 <sup>d,f</sup>	9	-	1	-	-				51	49						
8 <sup>d,f</sup>	10	-	1	-	-				12	88						
9 <sup>g</sup>	10	-	-	6	-					67	33					
10 <sup>g</sup>	11	-	-	6	-					23	77					
<i>Three-step sequences</i>																
11 <sup>e</sup>	3	10	15	4	yes	52	3	41			4					
12 <sup>h</sup>	8	5	10	6	-				65	30	2	3				
13 <sup>h</sup>	8	5	10	6	yes			5	72	21	2					
<i>Competitive reduction</i>																
14 <sup>c</sup>	2+3+5 7+10	10	15	6	yes	20	6	18	4	20	28	2	2	<1		
<i>Reductive amination</i>																
15 <sup>i</sup>	2	10	-	3	-							3	97			

<sup>‡</sup> Reported values were determined by GC-MS after a derivatization procedure and represent the average of at least two runs. Compounds **3** and **8** were not detected by this method and are thus omitted. See the Supplementary Information for additional control experiments, mean absolute deviations, and crude <sup>1</sup>H NMR spectra of selected reactions. <sup>a</sup>Unless otherwise specified: 1 M HCl in H<sub>2</sub>O, 16 h, 140 °C. <sup>b</sup>3 h, 140 °C. <sup>c</sup>3 h, 40 °C. <sup>d</sup>48 h, 140 °C. <sup>e</sup>20 °C, 24 h. <sup>f</sup>Reaction in 1 M H<sub>2</sub>SO<sub>4</sub> in H<sub>2</sub>O, 16 h, 140 °C. <sup>g</sup>1 h, 20 °C, 24 h, 140 °C. <sup>h</sup>Thermal cycling: 16 h, 140 °C; 10 h, 20 °C; 16 h, 140 °C. <sup>i</sup>Reaction with hydrazine hydrate (2 equiv), 1 M HCl in H<sub>2</sub>O, 80 °C, 16 h.